

## RESEARCH ARTICLE

# DNA methylation analysis of multiple imprinted DMRs in Sotos syndrome reveals *IGF2*-DMR0 as a DNA methylation-dependent, P0 promoter-specific enhancer

Hidetaka Watanabe<sup>1,2</sup> | Ken Higashimoto<sup>1</sup> | Noriko Miyake<sup>3</sup> | Sumiyo Morita<sup>4</sup> | Takuro Horii<sup>4</sup> | Mika Kimura<sup>4</sup> | Takayuki Suzuki<sup>5</sup> | Toshiyuki Maeda<sup>6</sup> | Hidenori Hidaka<sup>7</sup> | Saori Aoki<sup>1</sup> | Hitomi Yatsuki<sup>1</sup> | Nobuhiko Okamoto<sup>8</sup> | Tetsuji Uemura<sup>2</sup> | Izuho Hatada<sup>4</sup> | Naomichi Matsumoto<sup>3</sup> | Hidenobu Soejima<sup>1</sup>

<sup>1</sup>Division of Molecular Genetics and Epigenetics, Department of Biomolecular Sciences, Faculty of Medicine, Saga University, Saga, Japan

<sup>2</sup>Department of Plastic and Reconstructive Surgery, Saga University Hospital, Saga, Japan

<sup>3</sup>Department of Human Genetics, Yokohama City University Graduate School of Medicine, Yokohama, Japan

<sup>4</sup>Laboratory of Genome Science, Biosignal Genome Resource Center, Institute for Molecular and Cellular Regulation, Gunma University, Maebashi, Japan

<sup>5</sup>Avian Bioscience Research Center, Graduate School of Bioagricultural Sciences, Nagoya University, Nagoya, Japan

<sup>6</sup>Department of Pediatrics, Faculty of Medicine, Saga University, Saga, Japan

<sup>7</sup>Department of Internal Medicine and Gastrointestinal Endoscopy, Faculty of Medicine, Saga University, Saga, Japan

<sup>8</sup>Department of Medical Genetics, Osaka Women's and Children's Hospital, Izumi, Japan

## Correspondence

Ken Higashimoto and Hidenobu Soejima, Division of Molecular Genetics and Epigenetics, Department of Biomolecular Sciences, Faculty of Medicine, Saga University, Saga 849-8501, Japan. Email: higashim@cc.saga-u.ac.jp (K. H.), soejimah@cc.saga-u.ac.jp (H. S.)

## Funding information

MEXT | Japan Society for the Promotion of Science (JSPS), Grant/Award Number: 16K09970, 17K08687, 19H03621 and 17H01539; Japan Agency for Medical Research and Development (AMED), Grant/Award Number: 17ek0109280h0001, 17ek0109234h0001, 17ek0109205h0001, JP19ek0109280, JP19dm0107090 and JP19ek0109301; Ministry of Health, Labour

## Abstract

Haploinsufficiency of *NSD1*, which dimethylates histone H3 lysine 36 (H3K36), causes Sotos syndrome (SoS), an overgrowth syndrome. DNMT3A and DNMT3B recognizes H3K36 trimethylation (H3K36me3) through PWWP domain to exert de novo DNA methyltransferase activity and establish imprinted differentially methylated regions (DMRs). Since decrease of H3K36me3 and genome-wide DNA hypomethylation in SoS were observed, hypomethylation of imprinted DMRs in SoS was suggested. We explored DNA methylation status of 28 imprinted DMRs in 31 SoS patients with *NSD1* defect and found that hypomethylation of *IGF2*-DMR0 and IG-DMR in a substantial proportion of SoS patients. Luciferase assay revealed that *IGF2*-DMR0 enhanced transcription from the *IGF2* P0 promoter but not the P3 and P4 promoters. Chromatin immunoprecipitation-quantitative PCR (ChIP-qPCR) revealed active enhancer histone modifications at *IGF2*-DMR0, with high enrichment

**Abbreviations:** ATCC, American Type Culture Collection; BWS, Beckwith-Wiedemann syndrome; ChIP-qPCR, chromatin immunoprecipitation-quantitative PCR; DMR, differentially methylated region; H3K27ac, H3 lysine 27 acetylation; H3K36, H3 lysine 36; H3K36me3, H3K36 trimethylation; HTR-8, HTR-8/SVneo; ICR, imprinting control region; MALDI-TOF MS, matrix-assisted laser desorption/ionization time-of-flight mass spectrometry; PCR, polymerase chain reaction; Pen/Strep, Penicillin/Streptomycin; qRT-PCR, quantitative RT-PCR; RT-PCR, reverse transcription PCR; siRNA, small interfering RNA; SoS, Sotos syndrome; TET1, ten-eleven translocation 1; TSS, transcription start site; WGA, whole genome amplification.

This is an open access article under the terms of the Creative Commons Attribution-NonCommercial License, which permits use, distribution and reproduction in any medium, provided the original work is properly cited and is not used for commercial purposes.

© 2019 The Authors. The FASEB Journal published by Wiley Periodicals, Inc. on behalf of Federation of American Societies for Experimental Biology

and Welfare (MHLW), Grant/Award Number: H29-nanchitou(nan)-ippan-025; National Center for Child Health and Development (NCCHD), Grant/Award Number: 26-13; Gunma University, Grant/Award Number: 16029

of H3K4me1 and H3 lysine 27 acetylation (H3K27ac). CRISPR-Cas9 epigenome editing revealed that specifically induced hypomethylation at *IGF2*-DMR0 increased transcription from the P0 promoter but not the P3 and P4 promoters. NSD1 knock-down suggested that NSD1 targeted *IGF2*-DMR0; however, *IGF2*-DMR0 DNA methylation and *IGF2* expression were unaltered. This study could elucidate the function of *IGF2*-DMR0 as a DNA methylation dependent, P0 promoter-specific enhancer. NSD1 may play a role in the establishment or maintenance of *IGF2*-DMR0 methylation during the postimplantation period.

#### KEYWORDS

Beckwith-Wiedemann syndrome, epigenome editing, genomic imprinting, histone modifications, *NSD1*

## 1 | INTRODUCTION

Sotos syndrome (SoS; MIM: 117550) is an overgrowth syndrome characterized by prenatal and postnatal overgrowth, advanced bone age, characteristic facial structure including large skull, acromegalic features, and pointed chin, and varying degrees of mental retardation.<sup>1-3</sup> SoS is caused by *NSD1* haploinsufficiency resulting from mutations or deletions.<sup>4,5</sup> Located at chromosome 5q35, *NSD1* encodes a SET domain histone methyltransferase that dimethylates nucleosomal histone H3 lysine 36 (H3K36).<sup>6,7</sup> Analysis of homozygous *NSD1* knockout mice revealed an essential role for *NSD1* in early postimplantation development, but unlike patients with SoS, heterozygous knockout mice did not display any obvious phenotypic abnormalities.<sup>8</sup> Endogenous expression of FLAG-tagged NSD1 in HCT116, a human colorectal carcinoma cell line, resulted in binding of NSD1 near various promoter elements and regulated multiple genes involved in various processes, such as cell growth, tumorigenesis, cancer, keratin biology, and bone morphogenesis.<sup>9</sup> However, the molecular mechanism underlying the phenotypes caused by *NSD1* defects remain largely unknown.

H3K36 trimethylation (H3K36me3) is converted from H3K36me2 by another histone methyltransferase, SETD2. H3K36me3 is recognized by the PWWP domain of de novo DNA methyltransferases DNMT3A and DNMT3B, guiding de novo methyltransferase activity to ensure methylome integrity.<sup>10,11</sup> H3K36me3 levels were found to be significantly decreased in lymphoblastoid cell lines established from SoS patients.<sup>12</sup> Mutations in *DNMT3A* and *SETD2* have been identified in patients with Sotos-like overgrowth syndromes, including Tatton-Brown-Rahman syndrome (TBRS; MIM: 615879).<sup>13,14</sup> In addition, it has been recently reported that H3K36me2 is required for the recruitment of DNMT3A and the maintenance of DNA methylation in intergenic regions.<sup>15</sup> As suggested by these findings, genome-wide DNA methylation analysis in SoS patients with *NSD1* defects showed hypomethylation at thousands of CpG sites.<sup>16,17</sup> In addition,

*NSD1* mutations were identified in patients with Beckwith-Wiedemann syndrome (BWS; MIM: 130650), a distinct overgrowth syndrome; further, anomalies at 11p15, a disease locus for BWS, were identified in patients with SoS.<sup>18</sup> BWS is an imprinting disorder characterized by overgrowth, macroglossia, abdominal wall defects, and predisposition to embryonal tumors.<sup>19-21</sup> BWS is caused by dysregulation of imprinted genes within the *IGF2/H19* or *CDKN1C/KCNQ1OT1* imprinted domains at 11p15.<sup>19-21</sup> *IGF2* is an imprinted gene with paternal expression, and biallelic expression of *IGF2* caused by gain of methylation at imprinting control region 1 (ICR1) within the *IGF2/H19* domain is one of the causative alterations in BWS. Furthermore, DNMT3A and DNMT3B play pivotal roles in the establishment of imprinted differentially methylated regions (DMRs).<sup>22,23</sup> Taken together, these findings suggest that imprinted DMRs are also hypomethylated in SoS patients with *NSD1* defects. However, no previous studies investigating DNA methylation of genome-wide DMRs in SoS patients have been reported.

In the present study, we explored the DNA methylation status of 28 imprinted DMRs in 31 SoS patients with *NSD1* defects. Hypomethylation of imprinted *IGF2*-DMR0 and *IG-DMR* was found in a substantial proportion of these patients. We also showed that *IGF2*-DMR0 was an enhancer for the *IGF2* P0 promoter: the activity of this enhancer was found to be reinforced by DNA hypomethylation and lead to increased expression of *IGF2*. These findings suggest that overexpression of *IGF2* may explain certain phenotypic similarities between SoS and BWS, such as overgrowth.

## 2 | MATERIALS AND METHODS

### 2.1 | SoS patients and controls

A total of 31 SoS patients with *NSD1* defects, consisting of 19 cases with point mutations and 12 cases with microdeletion, were analyzed in this study (Supplemental Table S1).

Subsets of these patients have been included in previously reported studies.<sup>24,25</sup> Normal children ( $n = 24$ , 12 boys and 12 girls, average age = 3.8 years, ranging from 0 to 8 years) were also analyzed as normal controls. This study was approved by the Ethics Committee for Human Genome and Gene Analyses of the Faculty of Medicine of Saga University and the Institutional Review Boards of the Yokohama City University School of Medicine. Informed consent was obtained from all recruited subjects.

## 2.2 | DNA isolation and bisulfite conversion

Genomic DNA was extracted from peripheral blood and cultured cells using the FlexiGene DNA Kit (Qiagen, Hilden, Germany) and the QIAamp DNA Mini Kit (Qiagen), respectively, according to the manufacturer's instructions. Bisulfite conversion was performed on 500 ng samples of genomic DNA using the EZ DNA Methylation Kit (Zymo Research, Irvine, CA, USA) and the converted DNA was eluted in 100  $\mu$ L of nuclease-free water.

## 2.3 | Methylation analysis by matrix-assisted laser desorption/ionization time-of-flight mass spectrometry (MALDI-TOF MS) and bisulfite pyrosequencing

The DNA methylation status of 28 imprinted DMRs were measured using a two-step approach. The first step was MALDI-TOF MS analysis using a MassARRAY system (Sequenom, San Diego, CA, USA), and the second step was bisulfite pyrosequencing. These 28 DMRs were previously confirmed to be differentially methylated in the peripheral blood of normal controls.<sup>26</sup> During the first step of the MALDI-TOF MS analysis, each DMR was amplified by bisulfite polymerase chain reaction (PCR) using a primer set containing a primer that added the T7 promoter sequence at the 5' end. In vitro transcription of the PCR product was performed using T7 RNA polymerase, and the transcript was subjected to uracil-specific cleavage with RNase A. MALDI-TOF MS analysis of the cleaved fragments produced signal pattern pairs indicative of non-methylated and methylated DNA. EpiTYPER software (Sequenom) analysis of the signals returned a methylation index (MI) ranging from 0 (0% methylation) to 1 (100% methylation) for each CpG unit, which contained one or more CpG sites. The average methylation of all analyzed CpG units within each imprinted DMR for a given patient was compared with the normal controls. Aberrant hypomethylation was defined as a situation where the MI of a patient was lower than the average MI of normal controls minus 0.1 (average  $-0.1$ ). Aberrant hypermethylation

was defined as a situation where the MI of a patient was higher than the average MI of normal controls plus 0.1 (average  $+0.1$ ). The methylation status of the DMRs identified as showing aberrant methylation through the initial MALDI-TOF MS analysis step were quantitatively measured through bisulfite pyrosequencing (second step) using QIAGEN PyroMark Q24 software (Qiagen) according to the manufacturer's instructions. The average methylation of all analyzed CpGs within each imprinted DMR was compared between each patient and the normal controls. Aberrant hypomethylation was defined as a situation where the methylation percentage of a patient was lower than the average methylation percentage of normal controls minus 15% (average  $-15\%$ ). Aberrant hypermethylation was defined as a situation where the methylation percentage of a patient was higher than the average methylation percentage of normal controls plus 15% (average  $+15\%$ ). All primer sets were validated for the quantitative capability in MALDI-TOF MS and pyrosequencing analysis using varying mixtures of the Human Methylated & Non-Methylated (WGA) DNA Set (Zymo Research): 0%, 25%, 50%, 75%, and 100% methylated DNA, and this validation confirmed that the DMRs of normal controls showed low standard deviations in methylation (Supplemental Tables S2 and S3). All primers used in this study are listed in Supplemental Table S4.

## 2.4 | Cell culture

The TCL-1 and HEK293 cell lines were kindly provided by Dr H. Seki, Saitama Medical Center, Saitama, Japan, and Dr K. Izuhara, Saga University, Saga, Japan, respectively. The HTR-8/SVneo cell line (HTR-8) was obtained from the American Type Culture Collection (ATCC, Manassas, VA, USA). TCL-1 cells were cultured in RPMI 1640 medium (Wako Pure Chemical Industries, Osaka, Japan) containing 10% FBS and 1% Penicillin-Streptomycin (Pen/Strep; Gibco, Gaithersburg, MD, USA). HTR-8 cells were cultured in RPMI 1640 containing 5% FBS and 1% Pen/Strep. HEK293 cells were cultured in high-glucose DMEM (Sigma-Aldrich, St. Louis, MO, USA) containing 10% FBS and 1% Pen/Strep.

## 2.5 | Luciferase assay

A luciferase assay was performed to investigate whether *IGF2*-DMR0 influences *IGF2* promoter activity, using the PicaGene Dual Sea Pansy Luminescence Kit (Toyo Ink, Tokyo, Japan). Human genomic fragments containing the P0, P3, and P4 promoter regions and *IGF2*-DMR0 were amplified by PCR using primers harboring appropriate restriction

sites at their 5' end and cloned into the PGV-B and PGV-E vectors (Toyo Ink). PGV-B vector is a promoter-less firefly luciferase reporter vector, and PGV-E vector contains an SV40 enhancer downstream of the firefly luciferase gene. The sequences of the inserted fragments in final constructs were confirmed by Sanger sequencing. The constructs were transfected into TCL-1, HTR-8, and HEK293 cells using Lipofectamine 2000 (Invitrogen, Carlsbad, CA, USA) according to the manufacturer's protocol. Cotransfection with the pRL-TK vector, which contains the thymidine kinase promoter upstream of the Renilla luciferase reporter gene (Toyo Ink) was used to normalize. The activities of both luciferase constructs were detected 48 hours posttransfection.

## 2.6 | Total RNA preparation and quantitative RT-PCR (qRT-PCR)

Total RNA from cell lines was prepared using ISOGEN II reagent (Nippon Gene, Tokyo, Japan) according to the manufacturer's instructions. The total RNA samples were treated with recombinant DNase I (Takara Bio, Kusatsu, Japan) and then reverse-transcribed to single stranded cDNA using ReverTra Ace reverse transcriptase (Toyobo, Osaka, Japan) with random primers in accordance with the manufacturer's instructions. The cDNA was amplified using THUNDERBIRD SYBR qPCR Mix (Toyobo) or TaqMan Fast Universal PCR Master Mix (Life Technologies, Carlsbad, CA, USA) and quantified using a StepOnePlus Real-Time PCR System (Life Technologies).  $\beta$ -actin (Life Technologies, #4326315E) was used for normalization.

## 2.7 | CRISPR-Cas9 epigenome editing

CRISPR-Cas9 epigenome editing system was used to induce demethylation specifically at *IGF2*-DMR0. The system is based on a modification of the dCas9-SunTag system and can achieve efficient recruitment of an anti-GCN4 scFv fused to the ten-eleven translocation 1 (TET1) hydroxylase, an enzyme that demethylates DNA on a target region.<sup>27</sup> Five guide RNAs were designed in order to demethylate *IGF2*-DMR0. The target sequences of the gRNAs are shown in Supplemental Figure S4. The dCas9-peptide array fusion, scFv-GFP-TET 1 catalytic domain, and all five gRNA vectors were cotransfected at a molar ratio of 1:2:4 into TCL-1, HTR-8, or HEK293 cells using Lipofectamine 2000, and then sorted into GFP-positive and GFP-negative fractions at 48 hours posttransfection using a FACSaria II fluorescence-activated cell sorter (BD Biosciences). Genomic DNA and total RNA were then extracted from the GFP-positive cells.

## 2.8 | NSD1 knockdown

For NSD1 knockdown, two independent ON-TARGETplus small interfering RNA (siRNAs) for *NSD1*, and the ON-TARGETplus Non-Targeting Pool of siRNAs as a negative control, were purchased from Dharmacon (Lafayette, CO, USA; #J-007048-08-0005, #J-007048-09-0005, and #D-001810-10-05). The siRNAs were transfected into TCL-1, HTR-8, or HEK293 cells using Lipofectamine 2000 according to the manufacturer's protocol. At 72 hours posttransfection, cells were harvested and analyzed. The siRNA target sequences of *NSD1* were as follows: siRNA#1, GAUCAAAGCCUUCAUCCAA; and siRNA#2, GCCGAGAGCUGUUGAGAAA.

## 2.9 | Histone extraction and Western blotting

Acid-extracted histones were prepared from cells as previously described, with minor modifications.<sup>28</sup> Histones were separated by sodium dodecyl sulfate-polyacrylamide gel electrophoreses (SDS-PAGE) in 15% acrylamide gels, transferred to polyvinylidene difluoride (PVDF) membranes, blocked in 5% nonfat milk in PBS plus 0.1% Tween 20, probed with primary antibodies, and detected with horseradish peroxidase-conjugated anti-rabbit secondary antibodies and Amersham ECL Prime Western Blotting Detection Reagent (GE Healthcare, Chicago, IL, USA). The primary antibodies were anti-H3 (Abcam, Cambridge, UK; ab1791), anti-H3K36me2 (Abcam, ab9049), and anti-H3K36me3 (Abcam, ab9050) antibodies. For quantitative analysis, band intensities of H3K36me2, H3K36me3, and H3 were measured on images obtained using an LAS3000 instrument (Fujifilm, Tokyo, Japan) and ImageJ software (NIH, Bethesda, MD, USA), and then the histone modification signal was normalized to the corresponding H3 signal.

## 2.10 | Chromatin immunoprecipitation

The chromatin immunoprecipitation (ChIP) was performed according to a protocol provided by Millipore, with some modifications. In brief, cells were cross-linked with 1% formaldehyde for 8 minutes at room temperature. Cross-linking was quenched by addition of 125 mM glycine. After harvesting cells, the pellet was suspended in SDS lysis buffer (1% SDS, 10 mM EDTA, 50 mM Tris-HCl pH 8.1) with protease inhibitor cocktail (Nacalai Tesque, Kyoto, Japan). The lysate was sonicated and diluted 10-fold with ChIP dilution buffer (0.01% SDS, 1.1% Triton X-100, 1.2 mM EDTA, 16.7 mM Tris-HCl pH 8.1, 167 mM NaCl) containing protease inhibitor

cocktail. The diluted lysate was incubated with anti-H3K4me1 (Abcam, ab8895), anti-H3K4me3 (Abcam, ab8580), anti-H3 lysine 27 acetylation (anti-H3K27ac) (Abcam, ab4729), anti-H3K36me2 (Abcam, ab9049), anti-H3K36me3 (Abcam, ab9050), and normal rabbit IgG (Millipore, #12-370) overnight at 4°C. Immune complexes were collected with protein A sepharose beads (GE Healthcare), which were preblocked with salmon sperm DNA and BSA for 1 hour at 4°C. The beads were washed and eluted with elution buffer (1% SDS, 0.1 M NaHCO<sub>3</sub>, 10 mM DTT). The elution was incubated at 65°C overnight to reverse the cross-linking after adjusting the NaCl concentration. The DNA was purified with a QIAquick PCR Purification Kit (Qiagen), amplified with THUNDERBIRD SYBR qPCR Mix, and quantified using a StepOnePlus Real-Time PCR System.

## 2.11 | Statistical analysis

The statistical significance was calculated using an unpaired *t* test. *P* values less than .05 were considered statistically significant.

## 3 | RESULTS

### 3.1 | *IGF2*-DMR0 and IG-DMR are frequently hypomethylated in SoS patients

We quantitatively measured the DNA methylation status at 28 imprinted DMRs in 31 SoS patients with *NSD1* defects using a two-step approach (ie, MALDI-TOF MS analysis followed by bisulfite pyrosequencing). The methylation status of the DMRs that were initially detected as showing aberrant methylation using MALDI-TOF MS analysis were quantitatively remeasured through bisulfite pyrosequencing. The results are summarized in Figure 1 (see Materials and Methods for the definition of aberrant methylation). Actual methylation data from the MALDI-TOF MS analysis and bisulfite pyrosequencing are shown in Supplemental Tables S2 and S3, respectively. As we expected, all aberrantly methylated DMRs showed hypomethylation (Figure 1). Among them, hypomethylation at *IGF2*-DMR0 (42%, 13/31) and IG-DMR (65%, 20/31) occurred most frequently (Figure 1).

### 3.2 | *IGF2*-DMR0 functions as an enhancer for the *IGF2* P0 promoter

*IGF2*-DMR0 was frequently hypomethylated in SoS patients and a molecular correlation between SoS and BWS has

previously been described.<sup>18</sup> Therefore, we turned our focus toward functional analysis of *IGF2*-DMR0 for the remainder of this study.

*IGF2*-DMR0, which is normally methylated on paternal allele, is located within the *IGF2* gene, which has five promoters (P1, P0, P2, P3, and P4) located in exons 1, 2, 4, 5, and 6, respectively (Figure 2A).<sup>29</sup> Among the five *IGF2* promoters, P1 shows liver-specific activity and biallelic expression (Supplemental Figure S1A)<sup>30</sup>; therefore, we predicted that *IGF2*-DMR0 affected any of the remaining four promoters. We employed luciferase assay to investigate the function of *IGF2*-DMR0. For this assay, we selected three cell lines considered to be representative of a variety of transcriptional states from over 10 available human cell lines previously obtained by our laboratory. The three cell lines selected were human trophoblast cell lines TCL-1 and HTR-8/SVneo (HTR-8), and human embryonic kidney cell line HEK293. In TCL-1, transcripts from P0, P3, and P4 were detected (Supplemental Figure S1A). In HTR-8 and HEK293, transcripts from P3 and P4 were detected, whereas transcripts from P0 were not (Supplemental Figure S1A). Since transcripts from P2 were not detected in any of these cell lines, we excluded P2 from this study (Supplemental Figure S1A). Expression levels of total *IGF2* and of P0, P3, and P4, were strikingly higher in TCL-1 than in HTR-8 and HEK293 (Supplemental Figure S1B-E). Although apparent activities of P3 and P4 have been previously reported,<sup>31,32</sup> the activity of P0 (P0a in Supplemental Figure S2A) was previously reported as very weak,<sup>29</sup> which we confirmed (Supplemental Figure S2A-C).

Precise active promoter regions were required to investigate the function of *IGF2*-DMR0 on these promoters. Therefore, we searched for putative regulatory elements around exon 2 using programs GPMiner and FPROM<sup>33,34</sup> and found a TATA box approximately 500 bp upstream of exon 2, which was not contained in P0a (Figure 2A). We designated this region as P0b and observed its apparent promoter activity (Supplemental Figure S2A,B,D).

We made six constructs using P0b, P3, and P4 promoter regions, with and without *IGF2*-DMR0, to investigate the impact of *IGF2*-DMR0 on these promoters (Figure 2B). Luciferase assay revealed that in TCL-1, *IGF2*-DMR0 caused a statistically significant enhancement of P0b activity by more than two-fold (Figure 2C). However, *IGF2*-DMR0 did not affect the activities of the P3 and P4 promoters (Figure 2D,E). Furthermore, in HTR-8 and HEK293, *IGF2*-DMR0 did not enhance the activities of any of the promoters (Supplemental Figure S3). These results were consistent with the promoter usage profiles of the three cell lines and indicate that *IGF2*-DMR0 functioned as an enhancer of the P0b promoter in a cell-type-specific manner.



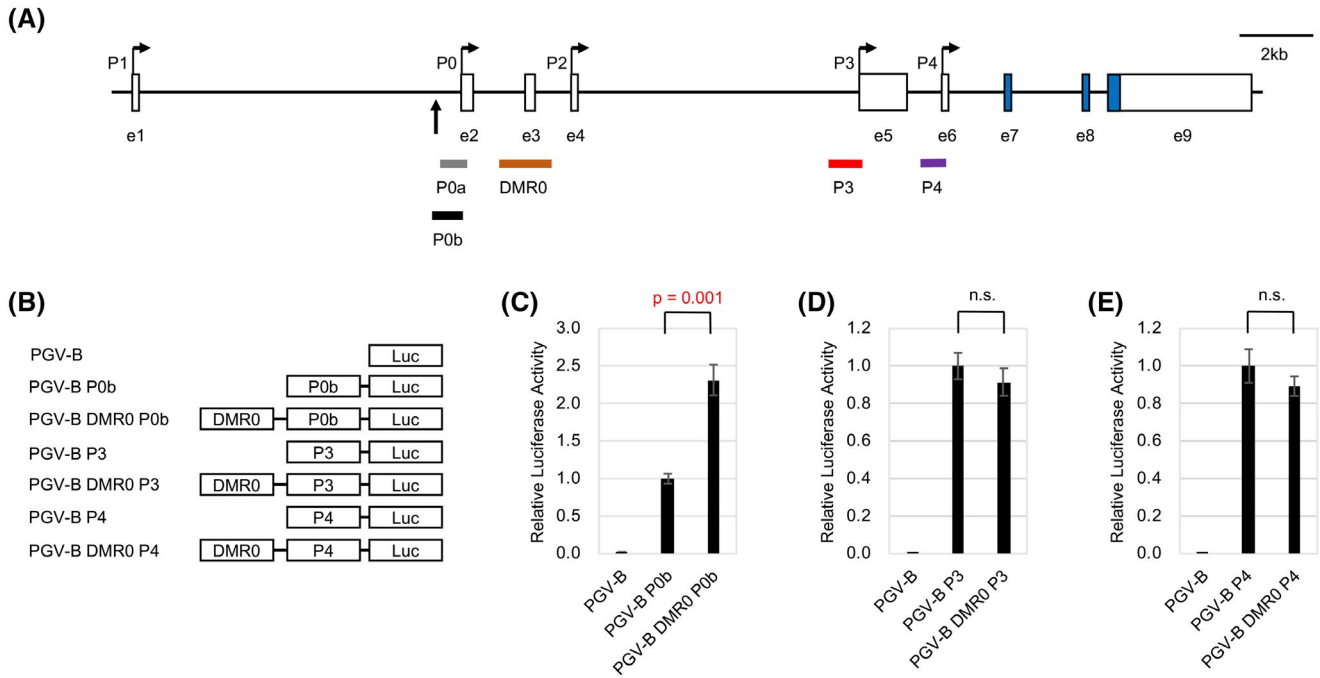


**FIGURE 2** *IGF2*-DMR0 enhances the P0 promoter activity of *IGF2* in TCL-1 cells. A, Schematic illustration of *IGF2* promoters. The broken arrows indicate the transcription start sites (TSSs) of each transcript from the P1, P0, P2, P3, and P4 promoters. The TSSs from P0, P3, and P4 were assigned based on GenBank accession numbers DQ104203.1, NM\_000612.6, NM\_001291861.2, respectively. *IGF2*-DMR0 is paternally methylated. Boxes indicate exons. Blue boxes indicate coding regions. The up-arrow shows the putative TATA box. The DNA fragments used in the luciferase assay are shown by thick horizontal lines. B, Structures of the constructs used in the luciferase assay. Luc: firefly luciferase gene. These constructs were transfected into TCL-1 cells along with a Renilla luciferase (pRL-TK) as an internal control. C, P0b activity was enhanced by *IGF2*-DMR0. The activity of PGV-B P0b was set to 1. D, P3 activity was unaffected by *IGF2*-DMR0. The activity of PGV-B P3 was set to 1. E, P4 activity was unaffected by *IGF2*-DMR0. The activity of PGV-B P4 was set to 1. Data represent mean values  $\pm$  SD of three independent experiments. n.s.: not significant

cells, while these modifications were relatively less present in the other two cell lines (Figure 3A,B). *IGF2*-DMR0 was significantly marked with H3K4me1 and H3K27ac, and weakly marked with H3K4me3, in TCL-1 cells; these modifications were relatively less present in the other two cell lines (Figure 3A,C). According to the chromatin state model reported by the NIH Roadmap Epigenomics Consortium, a region with strong enrichment for H3K4me1, H3K4me3, and H3K27ac is thought to be a promoter upstream from a transcription start site (TSS); a region with strong enrichment for H3K4me1 and H3K27ac, and weak enrichment for H3K4me3, is thought to be an active enhancer.<sup>35,36</sup> The ChIP-qPCR results for the P0 promoter and *IGF2*-DMR0 were consistent with the chromatin state model and the results of our luciferase assay. Therefore, we concluded that P0 was an active promoter upstream of a TSS and that *IGF2*-DMR0 was an active enhancer in TCL-1.

### 3.4 | DNA hypomethylation at *IGF2*-DMR0 enhances P0 promoter activity

Since hypomethylation at *IGF2*-DMR0 was found in about half of SoS patients, we examined whether *IGF2* expression was

altered by hypomethylation at *IGF2*-DMR0. We performed CRISPR-Cas9 epigenome editing to induce *IGF2*-DMR0-specific hypomethylation in TCL-1 cells<sup>27</sup> because *IGF2*-DMR0 was found to function as an active enhancer in TCL-1 but not in the other cell lines. We designed five guide RNAs and evaluated the methylation status of 12 CpG sites within *IGF2*-DMR0 using bisulfite pyrosequencing (Supplemental Figure S4). Epigenome editing was shown to reduce the average methylation of the 12 sites by approximately 15% without altering the methylation level at other DMRs, such as *IGF2*-DMR2, *H19*-DMR, and the *H19*-promoter, indicating successful induction of *IGF2*-DMR0-specific hypomethylation (Figure 4A, Supplemental Figure S5A). The reduction in the average methylation by epigenome editing was similar to the average reduction (approximately 20%) of *IGF2*-DMR0 observed in SoS patients with aberrant hypomethylation (Supplemental Table S3). qRT-PCR showed that this led to a two-fold increase in total *IGF2* expression compared with mock-edited control (Figure 4B). The expression level of the P0 transcript also increased two-fold, whereas the P3 and P4 transcripts were not altered (Figure 4B). We obtained the same results from two additional independent experiments (Supplemental Figures S5B,C and S6).

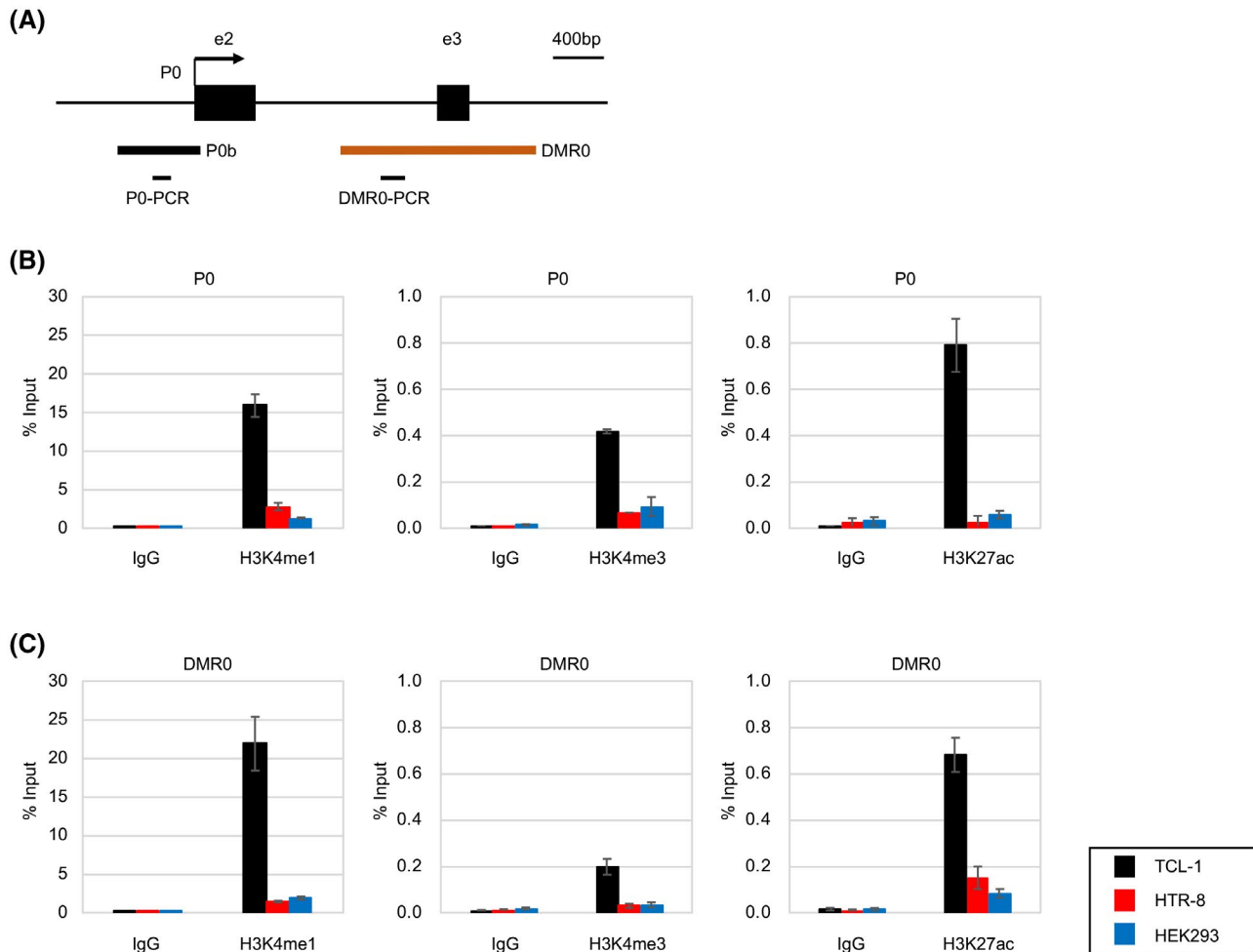


**FIGURE 3** Histone modification status at *IGF2* P0 promoter and *IGF2*-DMR0. A, Schematic illustration of *IGF2* P0 promoter and *IGF2*-DMR0. Regions analyzed by ChIP-qPCR are indicated by thin horizontal lines. B, Histone modification status of *IGF2* P0 promoter by ChIP-qPCR analysis in TCL-1 (black bar), HTR-8 (red bar), and HEK293 cells (blue bar). C, Histone modification status of *IGF2*-DMR0 by ChIP-qPCR analysis in TCL-1 (black bar), HTR-8 (red bar), and HEK293 cells (blue bar). The antibodies used are indicated below each graph. Normal rabbit IgG (IgG) was used as a negative control. Data represent mean values relative to input (% Input). Error bars represent the standard deviation ( $n = 3$ )

These results confirm that *IGF2*-DMR0 functioned as an enhancer and indicate that the enhancer activity of *IGF2*-DMR0 might be regulated by DNA methylation.

### 3.5 | NSD1 targets *IGF2*-DMR0 but does not influence its DNA methylation

Whether NSD1 targeted *IGF2*-DMR0 and whether NSD1 influenced its DNA methylation status still remained elusive. To investigate these points, knockdown of NSD1 was performed through transient transfection with either of two independent siRNAs targeting NSD1 (siRNA#1 and siRNA#2) or nontargeting siRNA (control) in the three cell lines. At 72 hours posttransfection, qRT-PCR indicated a significant reduction of *NSD1* mRNA expression (Figures 5A, 6A, Supplemental Figure S7A,D). To confirm knockdown

efficacy at the protein level, we employed Western blotting for H3K36me2 and H3K36me3 because there was no adequate, commercially available antibody against NSD1. The H3K36me2 level in whole cells decreased significantly, indicating successful NSD1 knockdown, while the H3K36me3 level remained unchanged (Figure 6A, Supplemental Figure S7A,D). At *IGF2*-DMR0, ChIP-qPCR revealed a significant reduction of H3K36me2 in all cell lines, whereas H3K36me3 was significantly reduced in TCL-1 and HTR-8 but not in HEK293 (Figure 5B,C). In addition, we measured the mRNA levels of *NSD2* and *NSD3*, which also encode H3K36 dimethyltransferases. Both *NSD2* and *NSD3* were expressed in all cell lines and their expression levels remained unchanged when NSD1 was knocked down (Supplemental Figure S8). The significant reduction in H3K36me2 observed under the NSD1 knockdown conditions suggested that NSD2 and NSD3 did not compensate for the depletion of NSD1, at least

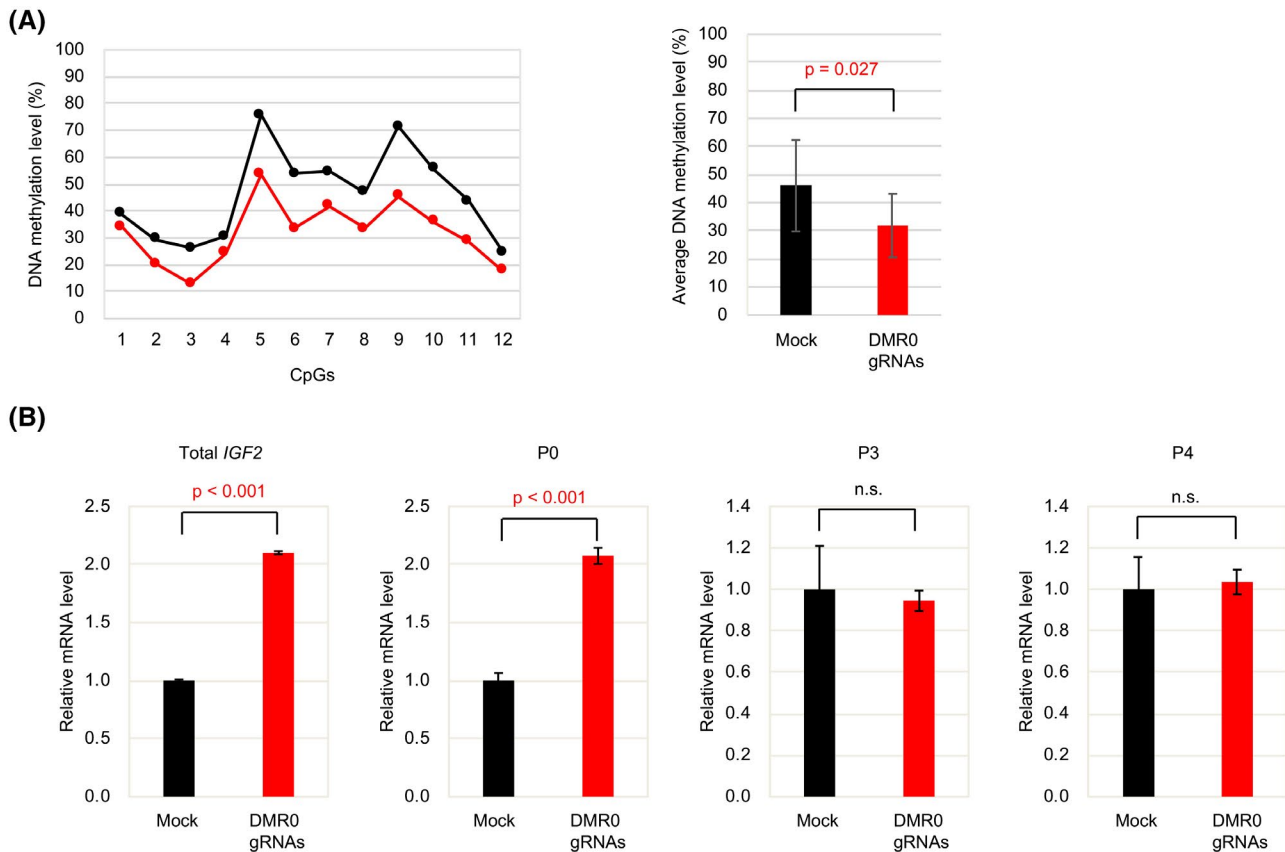


**FIGURE 4** *IGF2*-DMR0-specific hypomethylation induced in TCL-1 cells by CRISPR-Cas9 epigenome editing. Representative results of three independent experiments are shown (see Supplemental Figure S6). A, Left: Alteration of *IGF2*-DMR0 methylation by epigenome editing. The methylation level in cells transfected with all five gRNA vectors (DMR0 gRNAs) with dCas9-peptide array fusion and scFv-GFP-TET 1 CD (red). The empty gRNA vector was used as a control (mock, black). The methylation level of each CpG site was determined by bisulfite pyrosequencing. The number on the *x*-axis corresponds with the CpG number in Supplemental Figure S4. Right: The average methylation levels of analyzed CpGs. B, Comparison of *IGF2* mRNA level of total *IGF2*, and expression of transcripts from the P0, P3, and P4 promoters between mock-edited and DMR0 gRNAs by qRT-PCR analysis. Data were normalized to  $\beta$ -actin as an internal control. The mRNA level of mock-edited cells was set to 1. Error bars represent the standard deviation ( $n = 3$ ). n.s.: not significant

at *IGF2*-DMR0. Taken together, it is suggested that NSD1 constitutively targets *IGF2*-DMR0 and regulates the level of the H3K36me2 mark regardless of its enhancer activity; however, the effect of NSD1 on H3K36me3 may differ in a cell-type-specific manner.

We also examined the DNA methylation status of *IGF2*-DMR0 and the expression level of *IGF2* under NSD1 knockdown condition. *IGF2*-DMR0 methylation remained unaltered in all cell lines (Figure 6B, Supplemental Figure S7B,E), and the expression level of *IGF2* also remained unchanged. TCL-1, in which the P0 promoter and *IGF2*-DMR0 enhancer were active, showed no change in total *IGF2* and transcripts from P0, P3, nor P4 (Figure 6C). HTR-8 and HEK293, in which P0 was inactive, showed unchanged expression of total *IGF2* as well as P3 and P4 transcripts (Supplemental Figure S7C,F). The results of the NSD1 knockdown experiments indicate that DNA methylation of *IGF2*-DMR0 and *IGF2* expression were not influenced by NSD1, although NSD1 targeted *IGF2*-DMR0. Further, the

results of this study suggest that H3K36me2 and H3K36me3 are dispensable for the maintenance of DNA methylation at *IGF2*-DMR0, but that DNA methylation is essential for the enhancer function of *IGF2*-DMR0.

## 4 | DISCUSSION

In this study, we found that two imprinted DMRs, *IGF2*-DMR0 and IG-DMR, were frequently hypomethylated in SoS patients with *NSD1* defects. We also found that *IGF2*-DMR0 functioned as a P0 promoter-specific enhancer whose activity was essentially regulated by DNA methylation, but not by H3K36me, although NSD1 targets *IGF2*-DMR0.

The most important finding of this study was the elucidation of *IGF2*-DMR0. To date, the aberrant methylation of *IGF2*-DMR0 has been reported in imprinting disorders, namely BWS and Silver-Russell syndrome, as well as in several tumors.<sup>37-41</sup> The function of *IGF2*-DMR0, however, has

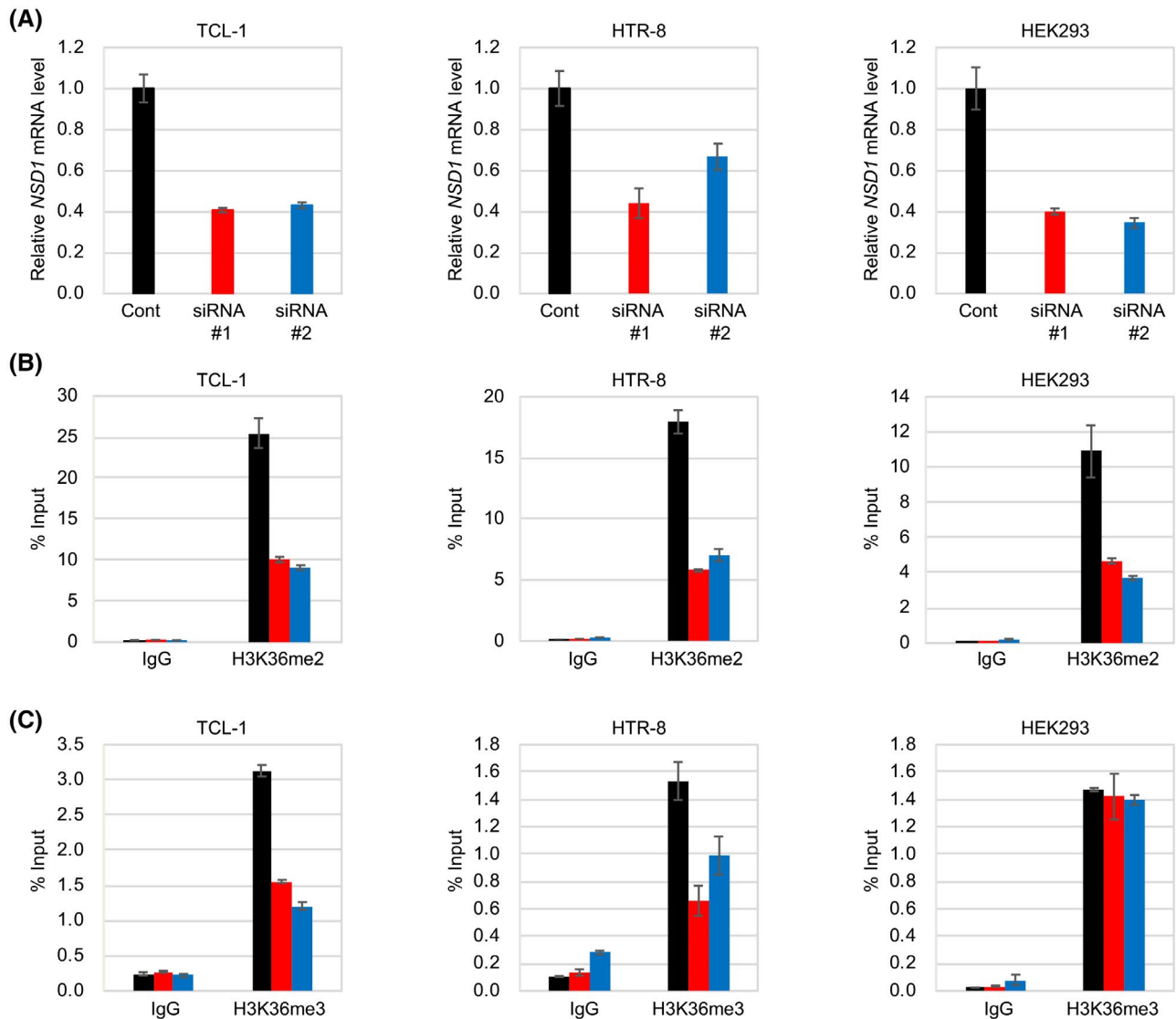


**FIGURE 5** Effect of NSD1 depletion on histone modifications of *IGF2*-DMR0. A, Decreased *NSD1* expression by siRNA. Two independent siRNAs (siRNA #1 and #2) targeting *NSD1* and nontargeting control siRNA (Cont) were transfected into TCL-1, HTR-8, and HEK293 cells. *NSD1* expression level was analyzed by qRT-PCR. Data were normalized to  $\beta$ -actin. The mRNA level of control cells was set to 1. Error bars represent the standard deviation ( $n = 3$ ). B, C, Effect of NSD1 depletion on H3K36me2 (B) and H3K36me3 (C) at *IGF2*-DMR0. H3K36me2 and H3L36me3 levels were analyzed by ChIP-qPCR. Each column shows data from control (black), siRNA #1 (red) and siRNA #2 (blue) transfected cells. The antibodies used are indicated below each graph. Normal rabbit IgG (IgG) was used as a negative control. The results are expressed as mean values relative to input (% Input). Error bars represent the standard deviation ( $n = 3$ )

remained obscure. Although there are structural similarities between the human and mouse homologs of the *IGF2* gene, there are also several differences. *Igf2*-DMR1 exists in mice but is absent in humans.<sup>29</sup> Transcripts from the P1 promoter show biallelic expression in the human liver, whereas they show paternal monoallelic expression in several mouse tissues.<sup>42</sup> *IGF2*-DMR0 shows sequence homology between human and mouse, and is located near the P0 promoter in both species. However, *IGF2*-DMR0 is paternally methylated in several human tissues, whereas it is specifically methylated on the maternal allele in mouse placenta.<sup>37</sup> The human P0 promoter is active in various fetal and adult tissues<sup>29</sup>; in

contrast, the mouse P0 is active only in the placenta.<sup>42</sup> These findings suggest that *IGF2*-DMR0 plays different roles in the regulation of *IGF2* expression in humans compared with mice. In this study, we found that human *IGF2*-DMR0 functioned as a P0 promoter-specific enhancer whose activity was regulated by DNA methylation. It is known that *IGF2* affects fetal and placental growth and birth weight.<sup>43,44</sup> In addition, the *Igf2* P0 transcript affects placental growth and nutrient transfer from mother to fetus via the placenta.<sup>45,46</sup> Taken together, these data strongly suggest that DNA hypomethylation at *IGF2*-DMR0 and subsequent overexpression of *IGF2* is one of the causative alterations for overgrowth in SoS. In

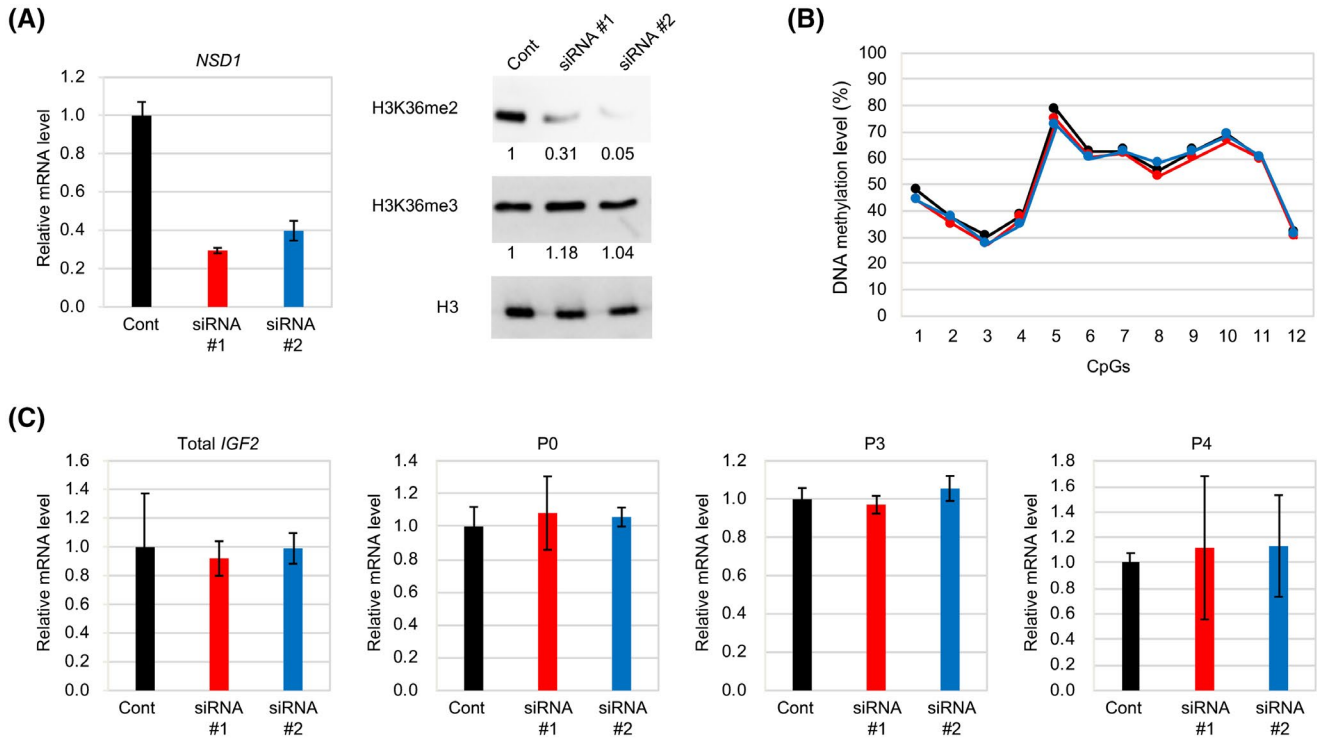


**FIGURE 6** Effect of NSD1 depletion on DNA methylation at *IGF2*-DMR0 and *IGF2* expression in TCL-1 cells. A, *NSD1* expression and H3K36me level on NSD1 depletion by siRNAs. Left: Decreased *NSD1* expression by siRNAs. Two different siRNAs (siRNA #1 and #2) targeted to the *NSD1* and nontargeting control siRNA (Cont) were transfected into TCL-1 cells. *NSD1* expression level in each cell was analyzed by qRT-PCR. Data were normalized to  $\beta$ -actin. The mRNA level of control cells was set to 1. Error bars represent the standard deviation ( $n = 3$ ). Right: Western blotting of H3K36me2 and H3K36me3. H3K36me2 decreased in NSD1 knockdown cells but H3K36me3 did not. Band intensity was quantified using ImageJ software. Data were normalized to Histone H3. The H3K36me level of control cells was set to 1. B, DNA methylation status of *IGF2*-DMR0 determined by bisulfite-pyrosequencing. The methylation level of each CpG in cells transfected with control siRNA, siRNA #1, and siRNA #2 are shown with black, red, and blue lines, respectively. The x-axis values correspond with the CpG numbers in Supplemental Figure S4. C, Comparison of *IGF2* mRNA level of total *IGF2*, and the transcripts from P0, P3, and P4 promoters between control siRNA, siRNA #1, and siRNA #2 by qRT-PCR. Data were normalized to  $\beta$ -actin. The mRNA level of control cells was set to 1. Error bars represent the standard deviation ( $n = 3$ ).

addition, overexpression of *IGF2* may explain certain phenotypic similarities between SoS and BWS, such as overgrowth.

*IGF2*-DMR0 is a somatic DMR. In mice, DNA methylation at somatic DMRs is established by Dnmt3b after implantation.<sup>47</sup> The PWWP domain of DNMT3B, like that of DNMT3A, recognizes the H3K36me3 mark, which is catalyzed by SETD2, the only enzyme that converts H3K36me2 to H3K36me3. This process results in deposition of the H3K36me3 mark within actively transcribed genes. Subsequently, binding of DNMT3B to the H3K36me3 mark leads to DNA methylation of transcribed gene bodies.<sup>11,48</sup> In our study, knockdown of NSD1 led to not only to decreased H3K36me2 levels at *IGF2*-DMR0 but also to decreased H3K36me3 levels at this site in a cell-type dependent manner. However, this decrease in H3K36me3 level did not influence the DNA methylation status of *IGF2*-DMR0. These results suggest that NSD1 was dispensable for the maintenance of this DMR in differentiated cells, because the TCL-1 and HTR-8 cell lines were established from full term and

first trimester placenta, respectively.<sup>49,50</sup> Since *IGF2*-DMR0 is established after implantation, we suppose that NSD1 may play a role in the establishment or the maintenance of *IGF2*-DMR0 methylation during the postimplantation period.

We also found hypomethylation of IG-DMR in a substantial proportion of SoS patients with *NSD1* defects. IG-DMR is a paternally methylated gametic DMR that functions as an ICR of the *DLK1-DIO3* imprinting domain. In addition, IG-DMR hierarchically regulates the methylation pattern of a somatic DMR, *MEG3*-DMR, in this domain.<sup>51</sup> This regulatory mechanism probably functions during the postimplantation period. Hypomethylation of IG-DMR is one of the causative alterations for Temple syndrome (TS, MIM 616222), a rare imprinting disorder.<sup>52,53</sup> Patients with TS caused by IG-DMR hypomethylation also show hypomethylation of *MEG3*-DMR,<sup>54</sup> indicating that IG-DMR hypomethylation leads to *MEG3*-DMR hypomethylation during the postimplantation period. In this study, however, all SoS patients with IG-DMR hypomethylation showed normal methylation

at *MEG3*-DMR. We considered that in SoS patients, DNA methylation at IG-DMR, which was normally established during spermatogenesis, was maintained until establishment of the *MEG3*-DMR methylation pattern after implantation. After the establishment of the *MEG3*-DMR methylation pattern, NSD1 defects might affect the maintenance of DNA methylation during the postimplantation period, leading to IG-DMR-specific hypomethylation. Since the *MEG3*-DMR methylation pattern is critical for imprinted gene expression and normal development of the body,<sup>51</sup> IG-DMR-specific hypomethylation may exert little influence on the clinical features of SoS. The frequent hypomethylation of *IGF2*-DMR0 and IG-DMR in patients with SoS has thus raised a question about a potential role of NSD1 in DNA methylation during the postimplantation period.

In conclusion, we found hypomethylation of *IGF2*-DMR0 and IG-DMR in a substantial proportion of SoS patients with *NSD1* defects. We could elucidate that *IGF2*-DMR0 functions as enhancer in regulating the expression of *IGF2* and that DNA demethylation of *IGF2*-DMR0 leads to an increase in *IGF2* expression. We propose that *IGF2* overexpression in SoS patients with *IGF2*-DMR0 hypomethylation may explain certain phenotypic similarities between SoS and BWS patients. However, we were unable to examine the role of NSD1 in DNA methylation using differentiated cell lines. The present findings suggest a role of NSD1 in DNA methylation (at least for *IGF2*-DMR0 and IG-DMR) during the postimplantation period. Further investigations using early developmental tissues from model mice, such as *NSD1* conditional knockout mice, are required to test this hypothesis.

## ACKNOWLEDGMENTS

We thank Dr H. Seki, Saitama Medical Center, Saitama, Japan, and Dr K. Izuhara, Saga University, Saga, Japan, for providing cell lines. We thank the Analytical Research Center for Experimental Sciences, Saga University, for their experimental support. This study was supported by the following: grants from the Grant-in-Aid for Scientific Research (C) program of the Japan Society for the Promotion of Science (16K09970, to KH; 17K08687, to HS; 19H03621, to N.Mi. (Noriko Miyake); 17H01539, to N.Ma. (Naomichi Matsumoto)), grants for Practical Research Projects for Rare/Intractable Diseases from the Japan Agency for Medical Research and Development (AMED) [17ek0109280h0001, 17ek0109234h0001, and 17ek0109205h0001, to HS; JP19ek0109280, JP19dm0107090, JP19ek0109301, JP19cm0106503, and JP19ek0109348, to N.Ma.), a grant for Research on Intractable Diseases from the Ministry of Health, Labor, and Welfare (H29-nanchitou(nan)-ippa-025, to HS), a grant for Child Health and Development Research from the National Center for Child Health and Development (26-13, to HS), and a grant from the Joint Research Program of the Institute for Molecular and Cellular Regulation at Gunma University (16029, to KH). We would

like to thank Uni-edit (<https://uni-edit.net/>) for editing and proofreading this manuscript.

## CONFLICT OF INTEREST

The authors declare that they have no competing interests.

## AUTHOR CONTRIBUTIONS

H. Watanabe, K. Higashimoto, and H. Soejima designed the study; N. Miyake, N. Matsumoto, and N. Okamoto collected the patient's samples; N. Miyake, N. Matsumoto performed *NSD1* mutation analysis; S. Morita, T. Horii, M. Kimura, and I. Hatada provided the plasmids for CRISPR-Cas9 epigenome editing system and supported the experiment; H. Watanabe and K. Higashimoto performed almost all experiments; S. Aoki, H. Hidaka, T. Maeda, and K. Higashimoto performed primers validation used for pyrosequencing and MassARRAY system; H. Watanabe, K. Higashimoto, T. Suzuki, H. Yatsuki, T. Uemura, and H. Soejima interpreted and discussed the results. H. Watanabe, K. Higashimoto, and H. Soejima wrote the paper. All coauthors participated in editing of manuscript drafts and have approved the final manuscript.

## REFERENCES

- Sotos JF, Dodge PR, Muirhead D, Crawford JD, Talbot NB. Cerebral gigantism in childhood. A syndrome of excessively rapid growth and acromegalic features and a nonprogressive neurologic disorder. *N Engl J Med.* 1964;271:109-116.
- Cole TR, Hughes HE. Sotos syndrome. *J Med Genet.* 1990;27:571-576.
- Cole TR, Hughes HE. Sotos syndrome: a study of the diagnostic criteria and natural history. *J Med Genet.* 1994;31:20-32.
- Kurotaki N, Imaizumi K, Harada N, et al. Haploinsufficiency of NSD1 causes Sotos syndrome. *Nat Genet.* 2002;30:365-366.
- Tatton-Brown K, Rahman N. Sotos syndrome. *Eur J Hum Genet.* 2007;15:264-271.
- Li Y, Trojer P, Xu CF, et al. The target of the NSD family of histone lysine methyltransferases depends on the nature of the substrate. *J Biol Chem.* 2009;284:34283-34295.
- Qiao Q, Li Y, Chen Z, Wang M, Reinberg D, Xu RM. The structure of NSD1 reveals an autoregulatory mechanism underlying histone H3K36 methylation. *J Biol Chem.* 2011;286:8361-8368.
- Rayasam GV, Wendling O, Angrand PO, et al. NSD1 is essential for early post-implantation development and has a catalytically active SET domain. *EMBO J.* 2003;22:3153-3163.
- Lucio-Eterovic AK, Singh MM, Gardner JE, Veerappan CS, Rice JC, Carpenter PB. Role for the nuclear receptor-binding SET domain protein 1 (NSD1) methyltransferase in coordinating lysine 36 methylation at histone 3 with RNA polymerase II function. *Proc Natl Acad Sci U S A.* 2010;107:16952-16957.
- Dhayan A, Rajavelu A, Rathert P, et al. The Dnmt3a PWWP domain reads histone 3 lysine 36 trimethylation and guides DNA methylation. *J Biol Chem.* 2010;285:26114-26120.
- Baubec T, Colombo DF, Wirbelauer C, et al. Genomic profiling of DNA methyltransferases reveals a role for DNMT3B in genic methylation. *Nature.* 2015;520:243-247.

12. Berdasco M, Ropero S, Setien F, et al. Epigenetic inactivation of the Sotos overgrowth syndrome gene histone methyltransferase NSD1 in human neuroblastoma and glioma. *Proc Natl Acad Sci U S A*. 2009;106:21830-21835.
13. Tatton-Brown K, Seal S, Ruark E, et al. Mutations in the DNA methyltransferase gene DNMT3A cause an overgrowth syndrome with intellectual disability. *Nat Genet*. 2014;46:385-388.
14. Tlemsani C, Luscan A, Leulliot N, et al. SETD2 and DNMT3A screen in the Sotos-like syndrome French cohort. *J Med Genet*. 2016;53:743-751.
15. Weinberg DN, Papillon-Cavanagh S, Chen H, et al. The histone mark H3K36me2 recruits DNMT3A and shapes the intergenic DNA methylation landscape. *Nature*. 2019;573:281-286.
16. Choufani S, Cytrynbaum C, Chung BH, et al. NSD1 mutations generate a genome-wide DNA methylation signature. *Nat Commun*. 2015;6:10207.
17. Aref-Eshghi E, Rodenhiser DI, Schenkel LC, et al. Genomic DNA methylation signatures enable concurrent diagnosis and clinical genetic variant classification in neurodevelopmental syndromes. *Am J Hum Genet*. 2018;102:156-174.
18. Baujat G, Rio M, Rossignol S, et al. Paradoxical NSD1 mutations in Beckwith-Wiedemann syndrome and 11p15 anomalies in Sotos syndrome. *Am J Hum Genet*. 2004;74:715-720.
19. Weksberg R, Shuman C, Beckwith JB. Beckwith-Wiedemann syndrome. *Eur J Hum Genet*. 2010;18:8-14.
20. Soejima H, Higashimoto K. Epigenetic and genetic alterations of the imprinting disorder Beckwith-Wiedemann syndrome and related disorders. *J Hum Genet*. 2013;58:402-409.
21. Brioude F, Kalish JM, Mussa A, et al. Expert consensus document: clinical and molecular diagnosis, screening and management of Beckwith-Wiedemann syndrome: an international consensus statement. *Nat Rev Endocrinol*. 2018;14:229-249.
22. Kaneda M, Okano M, Hata K, et al. Essential role for de novo DNA methyltransferase Dnmt3a in paternal and maternal imprinting. *Nature*. 2004;429:900-903.
23. Kato Y, Kaneda M, Hata K, et al. Role of the Dnmt3 family in de novo methylation of imprinted and repetitive sequences during male germ cell development in the mouse. *Hum Mol Genet*. 2007;16:2272-2280.
24. Kurotaki N, Harada N, Shimokawa O, et al. Fifty microdeletions among 112 cases of Sotos syndrome: low copy repeats possibly mediate the common deletion. *Hum Mutat*. 2003;22:378-387.
25. Kamimura J, Endo Y, Kurotaki N, et al. Identification of eight novel NSD1 mutations in Sotos syndrome. *J Med Genet*. 2003;40:e126.
26. Maeda T, Higashimoto K, Jozaki K, et al. Comprehensive and quantitative multilocus methylation analysis reveals the susceptibility of specific imprinted differentially methylated regions to aberrant methylation in Beckwith-Wiedemann syndrome with epimutations. *Genet Med*. 2014;16:903-912.
27. Morita S, Noguchi H, Horii T, et al. Targeted DNA demethylation in vivo using dCas9-peptide repeat and scFv-TET1 catalytic domain fusions. *Nat Biotechnol*. 2016;34:1060-1065.
28. Cheung P, Tanner KG, Cheung WL, Sassone-Corsi P, Denu JM, Allis CD. Synergistic coupling of histone H3 phosphorylation and acetylation in response to epidermal growth factor stimulation. *Mol Cell*. 2000;5:905-915.
29. Monk D, Sanches R, Arnaud P, et al. Imprinting of IGF2 P0 transcript and novel alternatively spliced INS-IGF2 isoforms show differences between mouse and human. *Hum Mol Genet*. 2006;15:1259-1269.
30. Ekstrom TJ, Cui H, Li X, Ohlsson R. Promoter-specific IGF2 imprinting status and its plasticity during human liver development. *Development*. 1995;121:309-316.
31. Ayesh B, Matouk I, Ohana P, et al. Inhibition of tumor growth by DT-A expressed under the control of IGF2 P3 and P4 promoter sequences. *Mol Ther*. 2003;7:535-541.
32. Lee SC, Min HY, Jung HJ, et al. Essential role of insulin-like growth factor 2 in resistance to histone deacetylase inhibitors. *Oncogene*. 2016;35:5515-5526.
33. Solovyev VV, Shahmuradov IA, Salamov AA. Identification of promoter regions and regulatory sites. *Methods Mol Biol*. 2010;674:57-83.
34. Lee TY, Chang WC, Hsu JB, Chang TH, Shien DM. GPMIner: an integrated system for mining combinatorial cis-regulatory elements in mammalian gene group. *BMC Genom*. 2012;13(Suppl 1):S3.
35. Roadmap Epigenomics C, Kundaje A, Meuleman W, et al. Integrative analysis of 111 reference human epigenomes. *Nature*. 2015;518:317-330.
36. Ernst J, Kellis M. Large-scale imputation of epigenomic datasets for systematic annotation of diverse human tissues. *Nat Biotechnol*. 2015;33:364-376.
37. Murrell A, Ito Y, Verde G, et al. Distinct methylation changes at the IGF2-H19 locus in congenital growth disorders and cancer. *PLoS ONE*. 2008;3:e1849.
38. Sullivan MJ, Taniguchi T, Jhee A, Kerr N, Reeve AE. Relaxation of IGF2 imprinting in Wilms tumours associated with specific changes in IGF2 methylation. *Oncogene*. 1999;18:7527-7534.
39. Cui H, Onyango P, Brandenburg S, Wu Y, Hsieh CL, Feinberg AP. Loss of imprinting in colorectal cancer linked to hypomethylation of H19 and IGF2. *Can Res*. 2002;62:6442-6446.
40. Hidaka H, Higashimoto K, Aoki S, et al. Comprehensive methylation analysis of imprinting-associated differentially methylated regions in colorectal cancer. *Clin Epigenetics*. 2018;10:150.
41. Sun F, Higashimoto K, Awaji A, et al. The extent of DNA methylation anticipation due to a genetic defect in ICR1 in Beckwith-Wiedemann syndrome. *J Hum Genet*. 2019;64(9):937-943.
42. Moore T, Constancia M, Zubair M, et al. Multiple imprinted sense and antisense transcripts, differential methylation and tandem repeats in a putative imprinting control region upstream of mouse Igf2. *Proc Natl Acad Sci U S A*. 1997;94:12509-12514.
43. Nordin M, Bergman D, Halje M, Engstrom W, Ward A. Epigenetic regulation of the Igf2/H19 gene cluster. *Cell Prolif*. 2014;47:189-199.
44. Moore GE, Ishida M, Demetriou C, et al. The role and interaction of imprinted genes in human fetal growth. *Philos Trans R Soc Lond B Biol Sci*. 2015;370:20140074.
45. Constância M, Hemberger M, Hughes J, et al. Placental-specific IGF-II is a major modulator of placental and fetal growth. *Nature*. 2002;417:945-948.
46. Sibley CP, Coan PM, Ferguson-Smith AC, et al. Placental-specific insulin-like growth factor 2 (Igf2) regulates the diffusional exchange characteristics of the mouse placenta. *Proc Natl Acad Sci U S A*. 2004;101:8204-8208.
47. Auclair G, Guibert S, Bender A, Weber M. Ontogeny of CpG island methylation and specificity of DNMT3 methyltransferases during embryonic development in the mouse. *Genome Biol*. 2014;15:545.
48. Morselli M, Pastor WA, Montanini B, et al. In vivo targeting of de novo DNA methylation by histone modifications in yeast and mouse. *eLife*. 2015;4:e06205.

49. Lewis MP, Clements M, Takeda S, et al. Partial characterization of an immortalized human trophoblast cell-line, TCL-1, which possesses a CSF-1 autocrine loop. *Placenta*. 1996;17:137-146.
50. Graham CH, Hawley TS, Hawley RG, et al. Establishment and characterization of first trimester human trophoblast cells with extended lifespan. *Exp Cell Res*. 1993;206:204-211.
51. Kagami M, O'Sullivan MJ, Green AJ, et al. The IG-DMR and the MEG3-DMR at human chromosome 14q32.2: hierarchical interaction and distinct functional properties as imprinting control centers. *PLoS Genet*. 2010;6:e1000992.
52. Ioannides Y, Lokulo-Sodipe K, Mackay DJ, Davies JH, Temple IK. Temple syndrome: improving the recognition of an underdiagnosed chromosome 14 imprinting disorder: an analysis of 51 published cases. *J Med Genet*. 2014;51:495-501.
53. Kagami M, Nagasaki K, Kosaki R, et al. Temple syndrome: comprehensive molecular and clinical findings in 32 Japanese patients. *Genet Med*. 2017;19:1356-1366.
54. Kagami M, Matsubara K, Nakabayashi K, et al. Genome-wide multilocus imprinting disturbance analysis in Temple syndrome and Kagami-Ogata syndrome. *Genet Med*. 2017;19:476-482.

## SUPPORTING INFORMATION

Additional supporting information may be found online in the Supporting Information section.

**How to cite this article:** Watanabe H, Higashimoto K, Miyake N, et al. DNA methylation analysis of multiple imprinted DMRs in Sotos syndrome reveals *IGF2-DMR0* as a DNA methylation-dependent, P0 promoter-specific enhancer. *The FASEB Journal*. 2020;34:960–973. <https://doi.org/10.1096/fj.201901757R>